Available online at www.sciencedirect.com
SCIENCE DIRECT®
Journal of Nuclear Materials 337–339 (2005) 510–514
journal of nuclear materials
www.elsevier.com/locate/jnucmat

Three-dimensional simulation of gas conductance measurement experiments on Alcator C-Mod

D.P. Stotler [a,*], B. LaBombard [b]

[a] *Princeton Plasma Physics Laboratory, Princeton University, James Forrestal Campus, P.O. Box 451, Rt #1 North Princeton, NJ 08543-0451, USA*
[b] *MIT Plasma Science and Fusion Center, NW17, Cambridge, MA 02139, USA*

Abstract

Three-dimensional Monte Carlo neutral transport simulations of gas flow through the Alcator C-Mod sub-divertor yield conductances comparable to those found in dedicated experiments. All are significantly smaller than the conductance found with the previously used axisymmetric geometry. A benchmarking exercise of the code against known conductance values for gas flow through a simple pipe provides a physical basis for interpreting the comparison of the three-dimensional and experimental C-Mod conductances.

PACS: 51.10.+y; 52.65.Pp
Keywords: Alcator C-Mod; Neutral modeling; DEGAS

1. Introduction

Monte Carlo simulations of the neutral gas behavior in the Alcator C-Mod divertor have yielded neutral pressures that are a factor of 10 smaller than those observed [1]. Lisgo et al. [2,3] has reduced the discrepancy to a factor of two by examining a variety of physics assumptions in the plasma and neutral transport models and by devising and applying improved models as needed. In particular, the approximate, axisymmetric representation of the neutral gas pathways through the three-dimensional (3-D) C-Mod sub-divertor has been found to be significantly inaccurate. Lisgo's results raise many questions, including how accurate are our neutral transport models?

Thoroughly validated and accurate neutral transport models will be needed to effectively assess the divertor performance of future burning plasma experiments. Detailed measurements of the gas conductance through the C-Mod vacuum vessel [4] provide an excellent opportunity to test these models. For the neutral pressures used in these measurements, typical of C-Mod discharges, the neutral gas transport is in the transition regime between molecular and viscous flow [2]. A 3-D, nonlinear Monte Carlo neutral transport code, like DEGAS 2 [5], should in principal be able to deal with flows of this type as well as treat the geometry in as much detail as is needed to replicate these experiments. We will evaluate its ability to do so and compare the resulting 3-D gas conductances with those obtained using an axisymmetric representation of the sort employed previously.

* Corresponding author. Tel.: +1 609 243 2063; fax: +1 609 243 2662.
E-mail address: dstotler@pppl.gov (D.P. Stotler).

0022-3115/$ - see front matter © 2004 Elsevier B.V. All rights reserved.
doi:10.1016/j.jnucmat.2004.10.091

2. Gas flow fundamentals

2.1. Two chamber model

For the purpose of defining the quantities of interest (see, for example, [6–8]), and to aid in the interpretation of the experimental and computational results, consider two volumes, V_1 and V_2, at pressures p_1 and p_2, connected by a narrow opening. A source of gas, Q_1, is introduced into the first volume and a sink, Q_2, in the second volume. Gas flows from the first volume into the second at a rate Q_{12} determined by the conductance of the opening

$$U_{12} = Q_{12}/(p_1 - p_2). \tag{1}$$

We first set the sink $Q_2 = 0$, take U_{12} to be a constant, and specify the pressures at $t = 0$. The time dependent solution of the equations describing this system has an initial transient that dies out for $t \gg V_1V_2/U_{12}(V_1 + V_2)$, leading to a steady pressure differential

$$p_1 - p_2 = \frac{1}{U_{12}}\frac{V_2Q_1}{V_1 + V_2}. \tag{2}$$

If we add a pump of speed S to the second volume so that $Q_2 = Sp_2$, we have instead steady state solutions

$$p_1 = Q_1\left(\frac{1}{S} + \frac{1}{U_{12}}\right), \quad p_2 = \frac{Q_1}{S}. \tag{3}$$

2.2. Physics model

The only atomic physics process in this paper is the elastic scattering of D_2 molecules off each other. An iterative, BGK treatment [9,10] is used with a reaction rate [11] $\langle\sigma v\rangle = k\ T/\eta$, where T is the gas temperature, and η is the experimentally measured viscosity.

Molecules striking material surfaces are absorbed and desorbed with 100% recycling. The desorbed molecules are sampled from a room temperature (300 K) Maxwell flux distribution. All gas sources have a room temperature Gaussian energy distribution with a cosine angular distribution.

2.3. Simple test case

We can validate the DEGAS 2 physics model and illustrate the change in conductance with flow regime by comparing the code with known conductances for a relatively simple geometry. Fluid flow regimes are characterized by the dimensionless ratio $K = \lambda/d$, the Knudsen number, where λ is the mean free path and d is a characteristic size of the cross section through which the gas is flowing [6]. For the D_2 elastic scattering process, $\lambda = 10^{-2}/p$ (Pa) m. In the 'molecular flow' regime, $K \gtrsim 1$, the molecules collide more frequently with the vessel walls than with each other. At the opposite extreme is the 'viscous flow' or 'continuum' regime, $K \lesssim 0.01$; it is subdivided into the 'viscous laminar' (for Reynolds number <1200, such as we have here) and 'turbulent' (Reynolds number >1200) regimes. Flows with $1 \gtrsim K \gtrsim 0.01$ are in the 'transition' regime.

We consider a 1 m long rectangular box divided into two volumes connected by a 0.205 m long (when run in the most convenient manner, the code used to set up this geometry yields zone sizes in this direction that are not quite round numbers), 0.1 m square pipe. The molecular flow conductance for this case is

$$U_{\mathrm{mf}} = A\frac{\bar{v}}{4}W, \tag{4}$$

where $A = 10^{-2}\mathrm{m}^2$ is the cross sectional area, $\bar{v}$ is the mean molecular velocity, $\bar{v}/4 = 314$ m/s, and $W = 0.38$ is the transmission probability through the pipe [6]. For a long pipe, laminar viscous flow is governed by the Poiseuille equation; the specific expression for the conductance of a rectangular pipe is [6]

$$U_{\mathrm{vf}} = \frac{1}{12\eta}\frac{a^2b^2}{L}\bar{p}Y, \tag{5}$$

where a, b are the sides of the opening, L is its length, $\bar{p}$ is the average of the pressures on either side of the opening, and $Y = 0.422$ is a numerical factor [6]. For the simulations presented here, the deviation from Poiseuille flow associated with finite pipe length [7] is $\lesssim 15\%$. The conductance in the transition regime can be described by an empirical fit due to Knudsen [6–8] that smoothly interpolates between the molecular and viscous flow expressions.

The conductances for five simulations are compared with Eqs. (4) and (5) in Fig. 1(a). We present these data as a function of Q_1 since it is an independent variable in the simulations, using Eqs. (1) and (3) to get $U_{\mathrm{vf}}(Q_1)$. The corresponding Knudsen numbers and the approximate bounds of the molecular and viscous flow regimes are shown in Fig. 1(b).

The two lowest Q_1 simulations are at or near the molecular flow regime. The conductance values for these two runs are within 2% of the expected value.

Knudsen's fit for the transition regime conductance is not directly applicable to these simulations. Instead, we show in Fig. 1(a), as an illustration, a smooth curve connecting the points computed from Eqs. (4) (for $Q_1 \leqslant 1\,\mathrm{Pa\,m^3/s}$) and (5) (for $Q_1 \geqslant 4\,\mathrm{Pa\,m^3/s}$).

In the viscous flow regime, the fluid velocity through the pipe is a maximum at the center and goes to zero at the walls, as is required by the 'no slip' boundary condition there. To determine whether or not we are adequately resolving this flow shear, two $Q_1 = 0.41\,\mathrm{Pa\,m^3/s}$ ($K \simeq 0.1$) runs have been done, one with 16 zones (smaller U_{12}) spanning the pipe and one with 64 zones. That different conductances result implies that spatial resolution of the flow is an issue. The higher U_{12} value is close

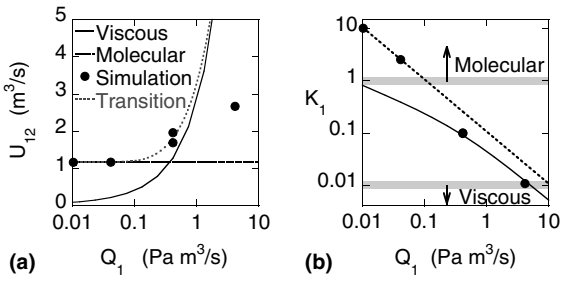

Fig. 1. (a) Comparison of simulated and reference conductances for a 0.205 m long, 0.1 m square pipe as a function of gas source strength. The 'transition' curve smoothly interpolates between the reference molecular and viscous flow results; it is intended to illustrate the expected variation of the conductance in the transition regime. The corresponding Knudsen numbers are shown in (b) with λ computed using p_1 and taking $d = 0.1$ m.

to the approximate 'transition' curve shown in Fig. 1(a), indicating that 64 zones may be sufficient in this case. The adequacy of 64 zones can only be determined by comparing with yet another run having even finer resolution.

The highest Q_1 simulation yields a lower than expected conductance, even though it likewise has 64 zones spanning the opening. As is shown in Fig. 1(b), the simulated $p_1 = 9.60$ Pa does not differ greatly from the expected value of 8.50 Pa. However, the simulated pressure drop $p_1 - p_2 = 1.55$ Pa is much larger than the 0.38 Pa corresponding to the viscous flow conductance. We expect that increasing the spatial resolution in the simulation will yield a smaller pressure drop and, consequently, a higher conductance.

3. Experimental conductance values

A set of gas-puff capillaries and in situ pressure gauges have been installed in Alcator C-Mod to permit the measurement of gas flows and conductances through the divertor structures [4] considered in [1,2]. We will focus on the gas flow through 'closed' and 'open' ports. In the former, the principal gas pathway between the main chamber/divertor and the divertor plenum ('gas box')/bottom pumping port volumes is a small slot underneath the outer divertor. In an 'open' port, the divertor tiles and support structure enclosing the gas box have been removed to facilitate diagnostic access.

The gas source, situated at the bottom outer edge of the gas box (Fig. 2), is calibrated by dividing the rate of rise of the main chamber neutral pressure by the torus volume. The volume V_1 corresponds to the gas box and bottom port; V_2 corresponds to everything else. In the simulations described in Section 4, $V_1 = 1.5 \times 10^{-2}$ m^3 and $V_2 = 2.8$ m^3. With these values, the time-scale of

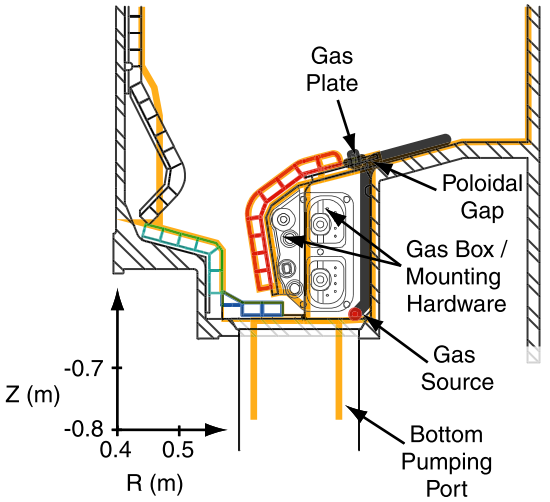

Fig. 2. The plane polygons used to construct the 3-D DEGAS 2 Alcator C-Mod geometry, shown in orange, are overlaid on an engineering drawing of the actual C-Mod lower divertor cross section [4]. Note that the latter shows the previous configuration for the inner divertor; the DEGAS 2 representation is derived from the current configuration.

the transient mentioned in Section 2.1 is on the order of milliseconds, much less than the 1–2 s over which the pressures are measured. Since $V_1 \ll V_2$, Eq. (2) is equivalent to Eq. (1).

The pressure p_1 is provided by a gauge at the bottom of the port below the gas capillary, and p_2 is given by a gauge adjacent to the main chamber. These pressure values rise uniformly while the capillary is open, but their difference, and hence the conductance, remains fairly constant. The gas flow is, thus, at or near the molecular flow regime. In the 'closed' divertor case, the bottom port pressure climbs from 2.9 to 3.6 Pa; the main chamber pressure starts at 1.1 Pa and finishes at 2.0 Pa, yielding an equilibrium conductance of 1.2 m^3/s. When the analogous experiment is performed at an 'open' port, the bottom pressure goes from 1.3 to 2.0 Pa while the main chamber pressure increases from 0.8 to 1.7 Pa. The equilibrium conductance in this case is 4.5 m^3/s.

4. Alcator C-Mod simulations

The toroidal variation of the C-Mod vacuum vessel and divertor hardware can be roughly described by a 'pie slice' model in which the various structures are represented as plane figures revolved about the major axis of the torus through a range of toroidal angles. Such a representation can be handled by a modest extension of the existing 2-D geometry setup tools used with DEGAS 2 [1].

Some of the plane 'polygons' we use are overlaid on a drawing of the actual C-Mod hardware in Fig. 2 [4]. Only a small portion of the entire geometry is shown so that we can focus on the divertor structures of interest. For a more detailed description of these structures, see [2]. Note also that the radial width of the vertical pumping ports has been reduced to match the cross sectional area of the actual port shape.

Most of the toroidal variation is associated with the pumping ports, the outer divertor plates/tiles, and the divertor mounting hardware/gas boxes. The pumping ports are treated as vacuum regions 6° wide, extending vertically to $Z = \pm 1.9$ m, at toroidal locations corresponding to each of the 10 C-Mod bays. The divertor mounting hardware (including the plates that support it) are modeled as 6° solid regions on either side of these ports; at other toroidal angles these volumes, the 'gas boxes', are treated as vacuum. In Fig. 2, the mounting hardware and its supporting plate are represented by two polygons (indicated by the arrows). The outer divertor plates and tiles are present everywhere except at the five 'open' bays that are spanned by a 6° vacuum gap. At the other five 'closed' bays, there is also a narrow, 3 mm gap that allows for thermal expansion. Following Lisgo [2], we include a small poloidal gap of either 0, 2, or 4 mm at the top of the gas box to simulate the effect of holes in the insulating material that fills the space between the gas plate and vacuum vessel.

A toroidally localized gas-puff source is specified at the bottom edge of the gas box. Since these DEGAS 2 simulations need to be time independent, we establish a pumping surface with an albedo of 90% at the top of the upper pumping ports.

The results from some of the runs are summarized in Table 1. For comparison, we include data from an axisymmetric simulation carried out with a geometry analogous to the 'closed bypass' case described in [1]. As in the experiment, the pressure p_1 is measured near the bottom of the pumping port below the gas source. The value of p_2 is taken near the outer wall of the main chamber. The estimated statistical error in the conductance (last column of the table) exceeds that of the individual pressures (a few percent or less) since the conductance is inversely proportional to their difference.

Table 1
Results from Alcator C-Mod simulations

Run	p_1 (Pa)	p_2 (Pa)	Q_1 (Pa m^3/s)	U_{12} (m^3/s)	Error (%)
Axisymmetric	0.21	0.16	1.99	40.	6.0
Open	1.46	1.22	1.86	7.8	16
Closed (base)	3.7	1.29	1.99	0.83	8.6
2 mm pol. gap	3.9	1.30	1.99	0.76	3.9
Reduce source	0.26	0.085	0.124	0.71	2.8

The closed port base run for the variations uses a 4 mm gap at the top of the gas box. The last column contains an estimate of the statistical error in the conductance.

The conductance in the 'open' port simulations is *larger* than the measured value of 4.5 m^3/s. Because the pressure differential is smaller in this run than in the 'closed' port cases, more flights have been used to increase the precision; the observed discrepancy is unlikely to be the result of Monte Carlo noise.

The conductance in the baseline 'closed' port simulation is *smaller* than the measured value of 1.2 m^3/s. Decreasing the poloidal gap from 4 to 2 mm lowers the conductance slightly. Three runs not included in Table 1 are worth mentioning briefly, but do not merit the space required to describe them adequately. First, removing the poloidal and narrow toroidal gaps entirely yields a much smaller conductance, $\sim$0.5 m^3/s. Second, two runs in which the sink strength and location are varied yield main chamber pressure changes consistent with Eq. (3); the conductance is not noticeably altered in either case.

5. Discussion

Our first conclusion is that fully detailed 3-D simulations of molecular and transition regime gas flows in fusion devices are possible and, in some cases, practical given the availability of relatively inexpensive massively parallel computers. For example, the baseline closed port case took 41 h on 30 1.7 GHz AMD Athlon processors (29 slaves plus 1 master). The number of 'flights' was increased gradually during the 30 iterations comprising the run, reaching 10^5 flights on the last iteration. The problem volume consisted of 56 659 computational zones.

To compare the axisymmetric result with the 3-D conductances, we imagine spreading the source uniformly amongst the 10 C-Mod bays. We can compute an effective conductance using $\overline{p_1}$, the average of the 10 pressures we would find at each of the pumping ports i, $p_{1,i}$. These are determined using the conductances in Table 1, $U_{12,i}$ (which takes on two values according to whether port i is open or closed): $p_{1,i} = p_2 + Q_{1,i}/U_{12,i}$. This yields $\overline{p_1} = p_2 + \frac{Q_{1,i}}{10}\left(\frac{5}{U_{12,\mathrm{c}}} + \frac{5}{U_{12,\mathrm{o}}}\right)$ since there are five open and five closed ports. The main chamber pressure can be found as before, $p_2 = Q_2/S$. If we spread the source evenly amongst the 10 ports, $Q_{1,i} = Q_{1,\mathrm{tot}}/10$. Our effective, or average, conductance is then $\overline{U_{12}} \equiv Q_{1,\mathrm{tot}}/(\overline{p_1} - p_2) = 20/(1/U_{12,\mathrm{c}} + 1/U_{12,\mathrm{o}})$. Using the simulated (experimental) conductances, we find 15 (19) m^3/s. We thus conclude that the axisymmetric geometry is effectively much more 'open' than the actual 3-D geometry, explaining, at least in part [2,3], the too-low neutral pressures seen in [1]. The realism of the axisymmetric geometry could be improved by appropriately narrowing the slot used in [1] to mock up the leakage pathways between the gas box and main chamber.

The simulated 3-D 'open' and 'closed' port conductances are in comparatively better agreement with the experimental values of Section 3 [4]. Yet, the remaining differences merit closer examination. That the simulated 'open' conductance is too high while the 'closed' case is too low suggests that the differences may be due to not-simulated details in the geometry and experimental arrangement. The results of Section 2.1 urge us to consider also the nature of the gas flow in these simulations. Lowering the source strength by a factor of 16 yields only a slightly lower conductance, suggesting that the particle flow in the 'closed' port case is nearly molecular. The dimensions of these gaps range from 3×10^{-3} to $\sim 5 \times 10^{-2}$ m. Using p_1 from the baseline run yields $K \sim 0.05 \rightarrow 1$. In the 'open' case, $d \sim 6 \times 10^{-2}$ m, yielding $K = 0.1$.

This range of Knudsen numbers encompasses the $K = 0.1$ value corresponding to the $Q_1 = 0.4\,\mathrm{Pa\,m^3/s}$ simulations of Section 2.1 and Fig. 1. Since that case is sensitive to the spatial resolution of the opening, we suspect that the C-Mod simulations may be as well. These simulations used four zones in the toroidal direction to span the 6° ports; only one zone covered the 'closed' port's 3 mm toroidal gap. Additional runs will be done in the future to assess the sensitivity of the conductance to the level of toroidal, and poloidal, resolution.

Future refinements and extensions of the work described in [1–3] will first need to be sure that axisymmetric geometries provide a gas conductance comparable to that of the detailed, 3-D geometry. Second, the sensitivity of simulations to the spatial resolution of transition regime and viscous gas flows through gaps will need to be checked. Third, benchmarks against measurements like those of [4] should performed whenever such data become available.

Acknowledgments

This work supported by U.S. DOE Contracts DE-AC02-CHO3073 and DE-FC02-99ER54512.

References

[1] D.P. Stotler et al., J. Nucl. Mater. 290–293 (2001) 967.
[2] S.W. Lisgo, PhD thesis, University of Toronto, 2003.
[3] S. Lisgo et al., these Proceedings. doi:10.1016/j.jnucmat.2004.09.073.
[4] B. LaBombard, C.J. Boswell, Tech. Rep. PSFC/RR-03-6, Massachusetts Institute of Technology, Plasma Science and Fusion Center.
[5] D.P. Stotler, C.F.F. Karney, Contrib. Plasma Phys. 34 (1994) 392.
[6] L. Holland, W. Steckelmacher, in: J. Yarwood (Ed.), Vacuum Manual, E. & F. N. Spon, London, 1974.
[7] S. Dushman, Scientific Foundations of Vacuum Technique, 2nd Ed., John Wiley, 1962.
[8] J.F. O'Hanlon, A User's Guide to Vacuum Technology, 3rd Ed.., John Wiley, 2003.
[9] D. Reiter et al., J. Nucl. Mater. 241–243 (1997) 342.
[10] R.J. Kanzleiter et al., Phys. Plasmas 8 (2000) 5064.
[11] C. May, Tech. Rep. JUEL-3486, Forschungszentrum Jülich, in German, 1997.